Articles

Stopped-Flow Fluorescence Spectroscopy of a Group II Intron Ribozyme Reveals that Domain 1 Is an Independent Folding Unit with a Requirement for Specific Mg^{2+} Ions in the Tertiary Structure†

Peter Zhifeng Qin‡ and Anna Marie Pyle*,§

Department of Biochemistry and Molecular Biophysics and Department of Applied Physics, Columbia University, New York, New York 10032

Received October 24, 1996; Revised Manuscript Received February 11, 1997⊗

ABSTRACT: A stopped-flow fluorescence spectroscopic assay for RNA folding was used to monitor the association of a multicomponent ribozyme derived from group II intron ai5γ. In the presence of Mg^{2+}, association of a short fluorescein-labeled oligonucleotide substrate with intron domain 1 (D1) resulted in a unique fluorescein emission enhancement, which reflected ribozyme folding and substrate binding. It was found that substrate binding follows a simple bimolecular encounter model, with k_{on} approaching the rate of simple duplex formation. The K_d between substrate and D1 was determined to be 11 nM, which is in close agreement with the K_d obtained through oligonucleotide cleavage assays requiring catalytic domain 5 (D5). Ribozyme variants D13 and D135, which contain D3 and/or D5 attached to D1 in-cis, bound substrate with very similar K_d values, suggesting that D1 can fold independently and contains all residues important for ground-state binding to substrate. Both stopped-flow fluorescence assays and chemical modification footprinting data showed that, in all three ribozymes, Mg^{2+} was required and sufficient for folding. The rates of substrate association and the fraction of active ribozyme showed similar [Mg^{2+}] dependencies, indicating that folding and substrate binding in these three ribozymes are the result of similar processes involving specific, weakly bound Mg^{2+} ions. The apparent binding constants for the Mg^{2+} ions were found to be approximately 70 mM in each case. Together, these data show that D1 is an independent folding unit with respect to substrate binding and that specific Mg^{2+} ions are required for the formation of a distinct tertiary structure in group II introns.

The catalytic function of a large RNA molecule depends on correct formation of its tertiary structure (Pyle & Green, 1995). Although the secondary structures of most catalytic RNA molecules are known, understanding of their detailed tertiary structures is limited. The large sizes of many catalytic RNA molecules render them difficult to study using conventional techniques of NMR or X-ray crystallography (Pley et al., 1994; Cate et al., 1996; Varani et al., 1996). In addition to a general lack of structural data, little is known about the pathways of RNA folding and the thermodynamic forces that stabilize a unique three-dimensional form (Draper, 1996). One feature that makes this problem more tractable is that many large RNA molecules can be divided into domains that can spontaneously assemble into a functional structure (Doudna & Cech, 1995; Michels & Pyle, 1995; Pan, 1995). These domains can function in-trans as individual molecules that, when in a complex, recapitulate catalytic activity of the parent molecule. Many studies have shown that certain individual RNA domains can fold independently, serving as building blocks, or nucleation points for tertiary structure formation (Doudna et al., 1991; van der Horst et al., 1991; Murphy & Cech, 1993; Zarrinkar & Williamson, 1994; Doudna & Cech, 1995; Michels & Pyle, 1995; Pan, 1995). This has led to an important view that the folding pathway of an RNA can be defined by its independent folding domains and the interactions between them (Pyle & Green, 1995). Thus, identifying these independent folding units is the first step in understanding folding of an RNA.

Self-splicing group II introns have been found in the organellar genes of plants, lower eukaryotes and prokaryotes (Michel & Ferat, 1995). The group II intron secondary structure can be arranged into a set of six domains (Michel et al., 1989), of which domain 1 (D1)[1] and domain 5 (D5) are strictly required for catalytic activity (Pyle, 1996). Domain 3 (D3) is not required (Koch et al., 1992; Michels

† Supported by National Institutes of Health Grant GMR0150313, the Searle Scholars Foundation, and the Beckman Foundation.

* Correspondence should be addressed to A.M.P. at the Department of Biochemistry and Molecular Biophysics, 630 W. 168th Street, Columbia University, New York, NY 10032. Phone: (212) 305-5430. FAX: (212) 305-7932. E-mail: amp11@columbia.edu.

‡ Department of Applied Physics.

§ Department of Biochemistry and Molecular Biophysics.

⊗ Abstract published in *Advance ACS Abstracts,* April 1, 1997.

[1] Abbreviations: ai5γ, the fifth intron in the gene for the third subunit of cytochrome oxidase from *Saccharomyces cerevisiae*; D1, domain 1 of intron ai5γ; D5, domain 5 of intron ai5γ; D3, domain 3 of intron ai5γ; K_d, dissociation constant; k_{off}, off-rate of S from D1; k_{on}, on-rate for S binding to D1; K_{Mg}, apparent dissociation constant for Mg^{2+}; FAM, fluorescein phosphoramidite for 5′-labeling of oligonucleotides; FAM-S, oligonucleotide substrate labeled at the 5′-end with FAM; IBS1, IBS2, intron binding sites 1 and 2 (found on the substrate); EBS1, EBS2, exon binding sites 1 and 2 (found on the intron); HPLC, high-pressure liquid chromatography; DMS, dimethyl sulfate.

S0006-2960(96)02665-7 CCC: $14.00

Scheme 1

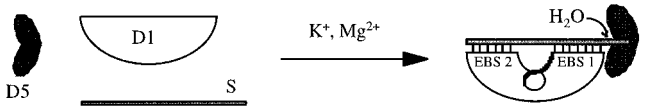

& Pyle, 1995), but it greatly enhances catalytic activity (Podar et al., 1995; Michels et al., 1997). In many RNA molecules, the apparent pattern of phylogenetic covariations between domains can be used to predict the overall tertiary organization of the molecule (Michel & Westhof, 1990). The group II intron represents a particularly interesting and challenging RNA folding problem because there are no phylogenetic covariations in Watson−Crick base pairing between the different catalytically important domains. Instead, interdomain architecture appears to be stabilized by a network of unusual tertiary interactions involving backbone residues and unusual base−base tertiary contacts (Chanfreau & Jacquier, 1994; Costa & Michel, 1995; Abramovitz et al., 1996). Although few of these interactions have been identified at this time, one approach to their characterization is the division of the parent RNA into separate domains. These individual domains can be manipulated as separate molecules, varying structure and concentration to probe the energetics of tertiary interactions.

In an effort to understand structure/function relationships in group II introns, a minimal ribozyme system was devised in which D1 and D5 were separated from the intron and reacted, in-trans, with oligonucleotide substrates (Michels & Pyle, 1995). The individual D1 and D5 RNAs bind and function together to carry out cleavage of RNA and DNA linkages (Griffin et al., 1995) within oligonucleotides that base pair to a set of "guide-sequences" within D1 (Scheme 1).

Detailed kinetic analysis of the reaction in Scheme 1 revealed that, in the presence of D5, the K_d between D1 and a short oligonucleotide substrate is 6.3 nM (Michels & Pyle, 1995). Because D1 includes the guide sequences, known as exon binding sites 1 and 2 (EBS1, 2), it is likely that a primary function of D1 is the recognition of substrate. However, in the secondary structure of D1, the two EBS regions lie far apart from each other (vide infra). To form the substrate binding site, the two EBSs must be brought together and be correctly aligned through the participation of other structural elements. This is supported by the observation that D1 deletion mutants containing only the EBS1 and 2 sites cannot bind substrate with high affinity (P.Z.Q. and A.M.P., manuscript in preparation). This implies that one or more folding events is a prerequisite for substrate binding and that the D1 folding problem can be linked experimentally to the kinetics of substrate binding.

To this end, a fluorescence spectroscopic assay was developed for studying the interactions of substrate with group II intron ribozymes. Using relatively simple instrumentation, fluorescence can be rapidly monitored under physiological conditions at low concentrations of sample (Lakowicz, 1983). Together with a stopped-flow apparatus, luminescence can be used to track ribozyme/substrate interactions directly and in real time (Bevilacqua et al., 1992). The *trans*-ribozyme system composed of D1, D5, and oligonucleotide substrate (S) was used for these first studies of D1 folding. In addition to being kinetically well-characterized (Michels & Pyle, 1995), the system also has the advantage that components can be manipulated independently with ease, both in-trans and in-cis. This allows one to study the interactions between domains by varying their concentration and structure.

Unlike proteins, where one can monitor an intrinsic fluorophore such as tryptophan, many RNA transcripts do not contain natural bases with a unique luminescence signature. Certain cellular RNA molecules have been post-transcriptionally modified in such a way that the luminescence properties of specific nucleotides have been enhanced (Leonard & Tolman, 1975). For example, the modified base 4-thiouridine absorbs and emits at longer wavelengths than A, G, C, or U (Shalitin & Feitelson, 1976). It was the presence of 4-thiouridine in natural $tRNA^{phe}$ that facilitated many studies on tRNA folding (Kayne & Cohn, 1974; Wolfson & Kearns, 1975; Milder et al., 1989). However, unless one wants to incorporate 4-thiouridine randomly or at every U position, it is difficult to place it at a specific position in an RNA molecule that has been transcribed in-vitro. In addition, RNA is very sensitive to UV damage at the wavelengths that induce intrinsic luminescence. Therefore, luminescence studies of large RNA transcripts require the addition of an extrinsic fluorophore that absorbs and emits light in the visible spectrum and does not damage the transcript through photochemical processes. An appropriate fluorescent label must be identified and placed in an informative position that does not disrupt the natural structure of the RNA (Kierzek et al., 1993; Tuschl et al., 1994). During the studies described herein, a fluorescein label was incorporated at the 5′ end of the oligonucleotide substrate. By following emission enhancement of this unique fluorophore, the interaction between substrate and D1 variants was tracked, allowing information on D1 folding to be derived. With this assay, the following questions have been addressed: Can D1 fold independently and bind substrate or does folding require the presence of other domains? How do metal ions promote the folding of D1? What is the role of D1 in folding of the entire intron?

MATERIALS AND METHODS

Preparation of 5′ Fluorescein-Labeled Oligonucleotide. The sequence of the substrate oligonucleotide is 5′ GUG GUGGGACAUUUUC˘GAGCG, with the underlined positions representing intron binding sites 2 and 1 (IBS2 and IBS1), respectively, and "˘" indicating the cleavage site. All oligonucleotides used in these experiments were synthesized on an Applied Biosystems 392 DNA/RNA synthesizer. 5′ Fluorescein labeling was carried out as the last coupling of the solid-phase synthesis, using the fluorescein dye phosphoramidite (FAM) from Applied Biosystems, Inc. (ABI). Deprotection of the oligonucleotide was carried out according to standard procedures (Wincott et al., 1995). Purification of the FAM-labeled substrate oligonucleotide (FAM-S) was carried out by reverse-phase HPLC on a Waters HPLC system fitted with a diode array detector, using a Nucleosil C18 column (250 mm × 4.6 mm) from Altech Associates, Inc. The gradient was run at 1.0 mL/min and ran from 10% to 30% buffer B in 30 min, with buffer A being 0.1 M triethylamine acetate (TEAA, from ABI) and buffer B being 100% acetonitrile. FAM-S was identified by the concurrence of absorbence peaks at 260 and 490 nm and eluted at around 22% buffer B. After the acetonitrile was evaporated by speedvac, fractions containing FAM-S

were precipitated with 0.3 M NaCl and 3× volume of 100% ethanol at −20 °C overnight. The oligonucleotide was resuspended in 10 mM 3-[*N*-morpholino]propanesulfonic acid (MOPS), pH 6.5, 1 mM EDTA, and stored at −20 °C. The concentration of the oligonucleotide was determined by absorbance at 260 nm in a Perkin Elmer Lambda 6 UV/vis Spectrophotometer. The extinction coefficient is 2.58×10^5 M^{-1} cm^{-1}, which takes into account the absorbance of fluorescein at 260 nm.

Preparation of Ribozymes. D1 and D5 were transcribed as described previously (Griffin et al., 1995; Michels & Pyle, 1995). Ribozyme D135 (584 nts) was transcribed from plasmid pT7D135 linearized with *Sca*I. This plasmid was constructed from plasmid pJD20 using Kunkel mutagenesis (Kunkel et al., 1991). Mutagenesis first replaced domains 2 and 4 with short stem loops. The 5′ exon was then removed and replaced with a T7 RNA polymerase promoter, so that the resulting RNA transcript starts at the first nucleotide of the ai5γ group II intron. Finally, a restriction site for *Sca*I was created between D5 and D6 to remove D6 from the RNA transcript. Ribozyme D13 (528 nts) was transcribed from plasmid pT7D13 linearized with *Bam*HI. This plasmid was constructed from plasmid pT7D123 (Griffin et al., 1995; Michels & Pyle, 1995) by replacing domain 2 with a short stem loop using Kunkel mutagenesis. Concentrations of each ribozyme were determined spectroscopically from absorbance at 260 nm, using an extinction coefficient of 1×10^4 M^{-1} cm^{-1} per nucleotide.

Oligonucleotide Cleavage Kinetics. Oligonucleotide substrate was 3′ end-labeled with ^{32}P using T4 RNA ligase (New England Biolabs) and radioactive cytidine 3′,5′-bis(phosphate) (pCp, MEN). Single-turnover reactions under saturating ribozyme concentrations were carried out as described previously (Griffin et al., 1995).

Chemical Modification and Reverse Transcription. In a procedure adapted from published work (Inouye & Cech, 1985; Pyle et al., 1992), approximately 2 pmol of D1 in 200 μL of buffer (0.08 M MOPS, pH 7.5, 0.5 M KCl or 0.1 M $MgCl_2$ as appropriate) was incubated at 42 °C for 30 min with or without 500 nM unlabeled substrate. Then 0.5 μL of dimethyl sulfate (DMS, Sigma) was added, and the reaction was incubated at 42 °C for 10 min. Reaction was stopped by addition of β-mercaptoethanol to 200 mM final concentration and ethanol precipitation. For reverse transcription, synthetic DNA primers were 5′ end-labeled with T4 kinase. For detection of modification sites, 0.5 pmol of modified D1 and 0.8−1.0 pmol of primer were dissolved in 7 μL of water and heated at 95 °C for 1 min. The temperature was gradually (over ∼1 h) reduced to 40 °C, and then 0.5 μL of 10 mM dNTPs, 2 μL of 5× buffer (250 mM Tris-HCl pH 8.5, 40 mM $MgCl_2$, 150 mM KCl, and 5 mM dithiothreitol), and 0.5 μL of AMV reverse transcriptase (25 units/μL, Boehringer Mannheim) were added. The reaction was incubated at 55 °C for 1 h and was then stopped by addition of an equal volume of quench buffer containing 7 M urea. Dideoxynucleotide sequencing of unmodified D1 was done in the same manner, except that reactions contained a 1:10 ratio of ddNTPs:dNTPs.

Spectroscopic Measurements. Each experiment was initiated with a standard preincubation procedure, designed to ensure that the RNA reaches a homogeneous state and to correct RNA misfolding that can occur during cold storage (Uhlenbeck, 1995). For the preincubation, all ribozymes were heated at 95 °C for 1 min in MOPS, pH 7.5. To avoid damaging the RNA, no Mg^{2+} was present during this heating process. After cooling the RNA solution to room temperature for two minutes, salts were added and the RNA was incubated in the following manner: Indicated amounts of ribozyme (D1, D13, or D135 at final concentration 25−200 nM) were added to a solution (1× buffer) containing 1 M KCl, 0.1 M $MgCl_2$, and 0.08 M MOPS, pH 7.5. This mix was incubated at 42 °C for 20 min. At the same time, FAM-S (final concentration 10 nM) was incubated in 1× buffer at 42 °C for 20 min. Binding was then initiated by rapid mixing in the stopped-flow apparatus or in a cuvette for steady-state measurements.

Steady-state emission spectra were measured in an Aminco-Bowman series 2 (AB2) luminescence spectrometer (SLM-Aminco). Luminescence of samples was measured in a 1 mL volume, and the temperature of the sample cell was maintained at 42 °C with a circulating water bath. The excitation wavelength was set at 490 nm. Stopped-flow measurements were done in an SLM-Aminco MilliFlow reactor, which was mounted on an SLM 48000S spectrophotometer. A xenon lamp was used as the light source, and the excitation wavelength was set at 490 nm. The emission signal was passed through a KV515 long-pass glass filter (from Schott Inc.) and measured with a photomultiplier tube (PMT). The observation cell (approximately 32 μL) and driving syringes (2.5 mL) were maintained at 42 °C with a circulating water bath. Reactants that had been preincubated under various conditions were loaded separately into the driving syringes. Reactions were initiated when the two components were driven and mixed into the stopped-flow observation cell by high-pressure gas. Data collection was triggered by an electronic signal as motion of the stop syringe was arrested by the adjustable stop, which was set at 90−100 μL to ensure reproducibility. The dead-time of the stopped-flow apparatus was determined to be 5 ms. Each measurement was repeated at least three times.

Pulse−Chase Experiments. FAM-S and D1 were incubated separately in 1× buffer as described above for 20 min. They were then combined, and incubation was continued at 42 °C for 5 min to ensure complete binding. Longer incubation times up to 20 min were checked, but binding was found to be fully equilibrated at 5 min. This pulse mix was then loaded into one of the driving syringes. At the same time, the chase mix, which contains excess unlabeled substrate in 1× buffer, was loaded into the other syringe. Initiation of the chase was then carried out as described above.

Data Analysis. Data from stopped-flow measurements were transferred into the curve fit program Kaleidagraph (Abelbeck Software). Data from each stopped-flow measurement were fit to a single exponential equation

$$f(t) = f_0 + f_1(1 - e^{k_{obs}(t)}) \quad (1)$$

where f_0 is the emission intensity at $t = 0$, f_1 is the magnitude of the fluorescence emission enhancement at $t = \infty$, and k_{obs} represents the apparent rate for the binding process. Values for k_{obs} from repeat measurements were averaged. Standard deviations from repeat measurements were between 5% and 25%, with most of them below 10%.

The dependence of k_{obs} on ribozyme concentrations was fit to a linear equation

$$k_{obs} = k_{on}[E] + k_{off} \quad (2)$$

where [E] represents the concentration of ribozymes D1, D13, or D135, and k_{on} and k_{off} are the on rate and off rate of S with respect to the ribozymes. The dependence of k_{obs} on Mg^{2+} concentrations was fit to the eq 5 in the text.

RESULTS

Evaluating FAM-S as a Probe for Folding of D1. Before ribozyme−substrate interactions could be measured spectroscopically, it was necessary to ensure that the fluorescent probe met two basic criteria. First, upon assembly of the system, the label would need to show adequate signal change. At the same time, to ensure that the information obtained through the label is an unbiased representation of the system, the label should minimally perturb activity of the ribozyme. To address the first issue, FAM-S was preincubated in reaction buffer and then combined with D1. Upon binding, the fluorescein emission intensity increased by around 15%, with no significant shift in the position of emission maxima (Figure 1a). Emission enhancement required covalent attachment of fluorescein to substrate and was specific to the ribozyme-bound form, as duplex formation between labeled substrate and its complementary strand did not give rise to such an enhancement (data not shown). The emission enhancement also required the presence of Mg^{2+} (vide infra). Taken together, these data indicate that the 5′ fluorescein label behaves as an appropriate probe for monitoring interactions between substrate and ribozyme.

Ribozyme perturbation by the 5′ fluorescein label was checked through two experiments. First, the single-turnover cleavage rates for FAM-S and the wild type substrate were compared. Under saturating ribozyme concentrations (100 nM D1, 3 μM D5), cleavage of FAM-S follows standard pseudo-first-order kinetics. The reaction rate for FAM-S is only 3-fold slower than that of the unlabeled substrate (Figure 1b). In energetic terms, this is a small rate effect, especially considering that fluorescein is a large probe incorporated near the active site. The high level of activity indicates that the 5′ fluorescein label has only minor effects on behavior of the ribozyme.

To determine whether bound FAM-S could be chased away from the complex and dissociate normally, a pulse−chase experiment was conducted in which the FAM-S/D1 complex was formed and then chased by the addition of unlabeled substrate in excess (Johnson, 1992; Kierzek et al., 1993). This experiment was necessitated by early results with a rhodamine-labeled substrate that was cleavable by the ribozyme (for one turnover) but which could not dissociate from the ribozyme active site (P.Z.Q. and A.M.P., unpublished results). This contrasts with behavior of FAM-S, which showed a decreased in emission intensity with time after addition of chase (Figure 1c). This indicates that the binding of FAM-S to D1 can be reversed by addition of unlabeled substrate, suggesting that these two substrates behave very similarly. Furthermore, the decrease in fluorescein emission during the pulse−chase process can be fit to a single exponential equation. The rate of decay was determined to be 0.25 ± 0.01 min^{-1}. Control experiments show that the decay rate is independent of the concentration of the competing oligonucleotide and FAM-S/D1 complex (Figure 1c, caption). This suggests that the rate is a measure of the k_{off} between labeled substrate and D1. As discussed later, the value of k_{off} from the pulse−chase experiment matches that determined by other methods.

Taken together, the data suggest that accurate information on interactions between substrate and ribozyme can be obtained by monitoring the spectroscopic properties of FAM-S. The fluorescein emission enhancement observed upon combining FAM-S with D1 provides the first evidence that D1 is able to bind substrate in the absence of other domains. Because D1 alone does not have catalytic activity, the affinity between S and D1 was previously inferred by monitoring the kinetics of substrate cleavage in the presence of other catalytic components, particularly D5 (Michels & Pyle, 1995). FAM-S therefore provides a way to study substrate binding independent of catalysis.

Dissociation/Association Kinetics of Substrate to D1. Having shown that FAM-S behaves like a normal substrate in steady-state experiments, we were able to extend studies of the interaction between substrate and D1 using stopped-flow spectroscopy, which allows one to track the interaction of substrate with D1 in real time (Johnson, 1992). Under both D1 excess and substrate excess conditions, the time traces of emission enhancement fit well to a single exponential equation (eq 1, Figure 2), indicating that association between substrate and D1 is a single-step process. That a multi-exponential equation did not result in best fit of the data suggests that the FAM-S and D1 reaction components behave as homogeneous entities and that there are no folding intermediates evident within the experimental timescale. Under D1 excess conditions, with the substrate concentration fixed at 10 nM, the k_{obs} values obtained from single exponential fits varied linearly with D1 concentration (Figure 2 inset). This is a strong indication that the binding of substrate to D1 can be described by a simple bimolecular encounter model shown in Scheme 2 (Fersht, 1985).

Scheme 2

$$S + D1 \underset{k_{off}}{\overset{k_{on}}{\rightleftharpoons}} S{\cdot}D1$$

In this model, the rate-limiting step is the association of the two components. Under conditions where one of the components is in excess, k_{obs} will show a characteristic linear dependence on the concentration of the excess component. The individual rates can be obtained by fitting the apparent observed rates (k_{obs}) to a linear equation (eq 2), where the slope represents the on-rate (k_{on}) of substrate binding to D1, and the *y*-intercept represents the off-rate (k_{off}). In this manner, it was determined that $k_{on} = (3.1 \pm 0.13) \times 10^7$ M^{-1} min^{-1} and $k_{off} = 0.33 \pm 0.15$ min^{-1} (Table 1).

The k_{on} of 3.1×10^7 M^{-1} min^{-1} is much smaller than the bimolecular rate of diffusional encounter (10^{11} M^{-1} min^{-1}; Eigen & Hammes, 1963). However, it is very close to the value of 10^7-10^8 M^{-1} min^{-1} that is typically observed for the formation of duplexes longer than three base pairs (Porschke & Eigen, 1971; Nelson & Tinoco, 1981; Herschlag & Cech, 1990). As substrate binding to D1 involves the formation of EBS·IBS helices, it is reasonable that the k_{on} obtained experimentally is limited by the rate of duplex formation. The k_{on} value reported here falls at the low end of the range known for the rate of duplex formation, so it is also possible that k_{on} is influenced by additional factors, such as the possibility of intramolecular hairpin formation within

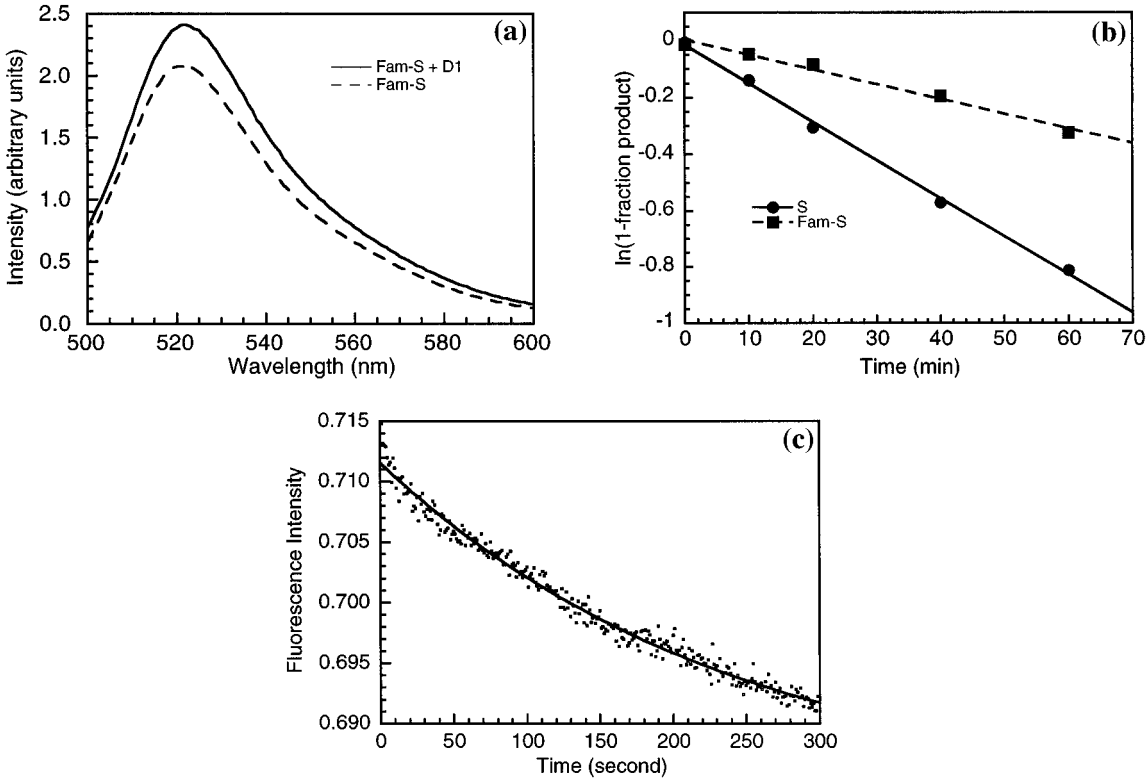

FIGURE 1: Applicability of FAM-S as a probe for D1 folding and substrate binding. (a) Steady-state fluorescence emission spectra of FAM-S. Emission spectra of 10 nM FAM-S in 1× buffer (1 M KCl, 0.1 M $MgCl_2$, 0.08 M MOPS, pH 7.5) were measured with and without D1 (100 nM). Measurements were done in an AB2 luminescence spectrometer (SLM-Aminco) with the excitation wavelength set at 490 nm. Each spectrum was measured three times and averaged. The background emission from the buffer was subtracted. Emission of FAM-S showed a 15% enhancement upon binding to D1, without change in the position of emission maxima. (b) FAM-S cleavage by the D1/D5 ribozyme. Cleavage rates for 3′-^{32}P end-labeled wild type substrate (S) and FAM-labeled substrate (FAM-S) were compared under standard reaction condition (1 M KCl, 0.1 M $MgCl_2$, 0.08 M MOPS, pH 7.5, 42 °C) with saturating ribozyme components (100 nM D1, 3 μM D5). The k_{obs} values for cleavage were (1.35 ± 0.04) × 10^{-2} min^{-1} for S and (0.520 ± 0.04) × 10^{-2} min^{-1} for FAM-S. The difference in cleavage rates was less than 3-fold, indicating that the FAM label did not disrupt the ribozyme active site. (c) Pulse−chase determination of FAM-S off-rate. After allowing 10 nM FAM-S and 50 nM D1 to bind for 5 min, 500 nM unlabeled substrate was added ($t = 0$ on this plot). Experiments were performed as described (Materials and Methods). The units of fluorescence intensity are arbitrary and depend on the gain setting of the PMT, which was held constant for repetitions of averaged experimental data. Five time traces were normalized to the same arbitrary intensity and then averaged. The averaged data were fit to a single exponential equation similar to eq 1. From this, the decay rate was determined to be 0.25 ± 0.01 min^{-1}. The decay rate were independent of the concentration of the competing oligonucleotide, for 100 nM unlabeled S, the rate = 0.24 ± 0.02 min^{-1}; for 1 μM unlabeled S, the rate = 0.29 ± 0.02 min^{-1}. The decay rate is also independent of D1/FAM-S concentration. When the [FAM-S] is increased to 20 nM, the decay rate was found to be 0.28 ± 0.02 min^{-1}. Thus, the decay rate represents the off-rate of FAM-S from D1.

the substrate. In any event, the slow on-rate is likely to be the rate-limiting step for binding and it will probably mask other processes, such as conformational change(s) in D1 that occur upon substrate binding. In the case of the *Tetrahymena* ribozyme derived from a group I intron, a docking process following duplex formation between ribozyme and substrate was detected by using very high labeled substrate concentration to overcome the slow duplex formation rate (Bevilacqua et al., 1992). As the emission enhancement of the fluorescein is limited in this system, it would be difficult to overcome k_{on} with large amounts of labeled substrate.

As k_{on} becomes limited by duplex formation, the strength of the binding interaction is determined mostly by k_{off}. The k_{off} obtained from the linear plot in Figure 2 is 0.33 min^{-1}. This is in good agreement with the rate determined from pulse−chase experiments (Figure 1c), thereby confirming that D1/substrate association can be modeled as a bimolecular collision.

The dissociation constant (K_d) between substrate and D1 was determined from the relationship $K_d = k_{off}/k_{on}$, and was calculated to be 11 ± 5.0 nM (Table 1). This is in close agreement with the 6.3 nM value obtained through kinetic cleavage assays in which D5, the catalytically essential component, was presented in-trans (Michels & Pyle, 1995). In the absence of D5, D1 loses catalytic activity, but the fluorescence results suggest that the binding strength of D1 to substrate is not weakened. It is remarkable that the K_d values measured for the S/D1 complex are so similar given that two completely different approaches were used in their determination. This strong similarity provides an additional assurance that the FAM label does not radically alter normal behavior of the substrate.

Binding Strength of D1 to Substrate Is Independent of Other Domains. To further test whether D1 can fold and bind substrate independently, the substrate binding affinity of two other ribozyme variants was measured. The first variant, D13, contains domain 1 and domain 3 (D3) connected by a short stem loop. The presence of D3 results in a ribozyme with a much faster cleavage rate (Michels et al., 1997), although D5 is still required for catalytic activity. Using the fluorescence assay, the k_{on} of substrate binding to D13 was measured to be (2.8 ± 0.097) × 10^7 M^{-1} min^{-1} and k_{off} = 0.12 ± 0.098 min^{-1}. This resulted in a K_d = 4.3 ± 3.5 nM (Figure 3, Table 1). Values of k_{on}, k_{off}, and K_d

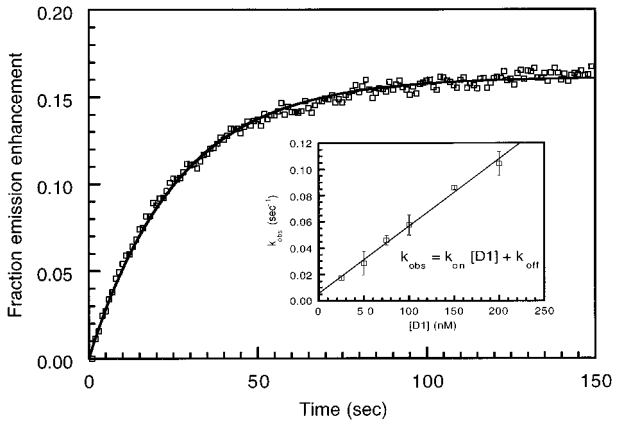

FIGURE 2: Stopped-flow kinetics of FAM-S binding to D1. Association of 10 nM of FAM-S with excess D1 was monitored in a stopped-flow apparatus as described (Materials and Methods). Data were fit to eq 1. The time trace shown was obtained using 50 nM D1, and a k_{obs} of 0.037 s^{-1} was observed. Inset: k_{obs} from repeat measurements were averaged, and plotted against D1 concentrations. Data fit very well to a linear equation (eq 2). From the fit, the following data were obtained: $k_{on} = (3.1 \pm 0.13) \times 10^7$ M^{-1} min^{-1}, $k_{off} = 0.33 \pm 0.15$ min^{-1}, and $K_d = k_{off}/k_{on} = 11 \pm 5.0$ nM. The numerical values shown for emission enhancement were normalized by subtracting each intensity at time (t) from the intensity at time = 0 and then dividing this value by the absolute intensity at time = 0.

Table 1: Rate Constants of Substrate Binding for Various Ribozymes[a]

ribozyme	k_{on} ($\times 10^7$ M^{-1} min^{-1})[b]	k_{off} (min^{-1})[b]	K_d (nM)[c]
D1	3.1 ± 0.13	0.33 ± 0.15	11 ± 5.0
D13	2.8 ± 0.097	0.12 ± 0.098	4.3 ± 3.5
D135	2.2 ± 0.12	0.45 ± 0.15	20 ± 7.1

[a] Values were obtained from fitting data in Figures 2 and 3. [b] Standard errors were obtained using the curve fit program Kaleidagraph (Abelbeck). [c] $K_d = k_{off}/k_{on}$. Errors calculated by propagation from k_{off} and k_{on} measurements.

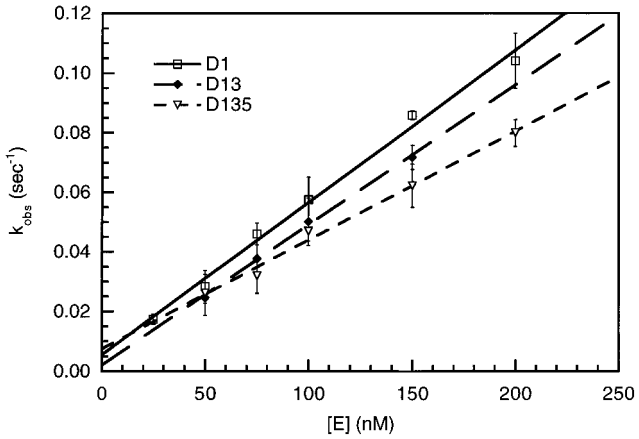

FIGURE 3: Concentration-dependent binding kinetics for ribozyme variants. Association rates of 10 nM FAM-S with ribozyme D1, D13, and D135 were measured and plotted against ribozyme concentration. For each ribozyme, the data fit very well to a linear equation (eq 2). Values for k_{on}, k_{off}, and K_d are provided in Table 1. The k_{obs} for each ribozyme was very similar at the same concentration, resulting in similar K_d values for all three ribozymes.

are all similar to those of D1. It seems that no extra energy in substrate binding is gained when D3 is attached to D1, even though the catalytic rate is enhanced. Therefore, correct configuration of the substrate binding site does not require D3.

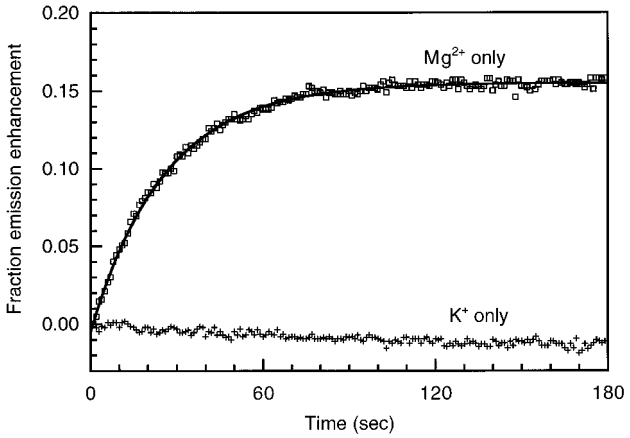

FIGURE 4: Dependence of D1 conformation on different metal ions. Association of 10 nM FAM-S and 50 nM D1 was monitored. Buffer contained 0.08 M MOPS, pH 7.5, 1 M KCl or 0.1 M $MgCl_2$, as indicated. In buffer containing 1 M KCl without Mg^{2+}, no emission enhancement was observed. In buffer containing 0.1 M $MgCl_2$ without K^+, emission enhancement was observed. The Mg^{2+} time trace showed maximum emission enhancement of 15% and a k_{obs} of 0.039 s^{-1}, which are the same as those in buffer containing Mg^{2+}/K^+ (Figure 2), suggesting that Mg^{2+} alone is sufficient for D1 to fold and bind substrate.

The effect of D5 on substrate binding was tested in two experiments. First, the k_{obs} value was measured spectroscopically in the presence of excess D5 in-trans (10 nM FAM-S, 50 nM D1, 1 μM D5) and was determined to be 0.0276 ± 0.0008 s^{-1}, which is nearly identical to the k_{obs} value of 0.0284 ± 0.009 s^{-1} observed in the absence of D5. Furthermore, association of FAM-S and the ribozyme variant D135, which has D1, D3, and D5 all connected in-cis, was tested. It was determined that for D135, $k_{on} = (2.2 \pm 0.12) \times 10^7$ M^{-1} min^{-1}, $k_{off} = 0.45 \pm 0.15$ min^{-1}, and $K_d = 20 \pm 7.1$ nM (Figure 3, Table 1). Again, these values are similar to those of D1 alone. Taken together, these data indicate that neither trans- nor cis-acting D5 contributes extra energy for substrate binding.

Role of Mg^{2+} in D1 Folding and Substrate Binding. Cleavage of oligonucleotides by the D1/D5 complex requires high concentrations of both Mg^{2+} and K^+, although certain other monovalents will substitute to a limited extent for K^+ (Michels, 1997). While it was known that metal ions were required for catalysis, it was not clear if they played an exclusive role in chemistry, or if they played an additional role in ribozyme folding. After all, not all ribozymes have been reported to require divalent metal ions for folding (Heus & Pardi, 1991; Smith et al., 1992; Pyle, 1993). It was therefore of interest to determine the salt requirements for D1 folding and substrate binding. When binding was initiated in a buffer that contains only 0.1 M $MgCl_2$, a fluorescein emission enhancement similar to that in $MgCl_2$/KCl buffer was observed (Figure 4) and the k_{obs} for this process was the same as that observed in the presence of KCl. Conversely, when the experiment was conducted in buffer containing only 1 M KCl, without $MgCl_2$, no fluorescein emission enhancement was observed (Figure 4). These data suggest that K^+ does not promote folding of a D1 molecule that is competent for substrate binding. In addition, they show that K^+ does not enhance the ability of Mg^{2+} to promote folding of the RNA. Instead, the data indicate that Mg^{2+} alone is sufficient for promoting the tertiary fold of D1 and that any requirement previously

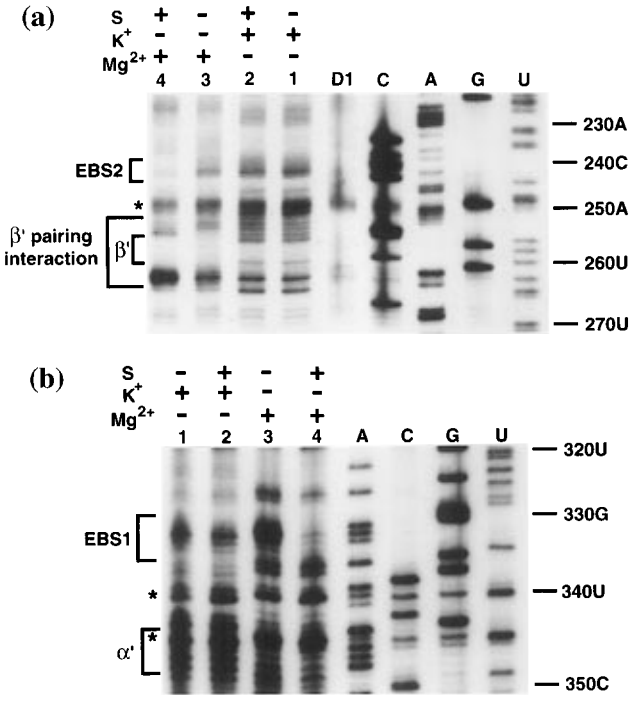

FIGURE 5: DMS modifications of D1. DMS modifications of D1 were done under various conditions as indicated, and visualized by reverse transcription (Materials and Methods). Primers complementary to nucleotides 335−358 (A) and nucleotides 405−423 (B) of group II intron ai5γ (with the 5′ first nucleotide being position 1) were used. Lanes U, G, A, and C: dideoxy sequencing of unmodified D1. Lane D1: primer extension of unmodified D1. Lanes 1−4: primer extensions of D1 modified under different conditions as indicated (S is 500 nM unlabeled substrate, K^+ is 0.5 M KCl, Mg^{2+} is 0.1 M $MgCl_2$). Primer extension stops one nucleotide before the modified base (Inouye & Cech, 1985). Nucleotide position numbers are given on the right. Locations of specific structural elements within D1 are indicated on the left. Asterisks indicate sites of DMS-independent reverse-transcriptase stops.

reported for K^+ was related to a potential role in binding of D5 or in the chemical step of catalysis. From a more conservative standpoint, the data may indicate that K^+ alone does not promote formation of the ribozyme fold that stimulates emission enhancement, regardless of whether or not substrate is bound. This is because K^+ might promote ribozyme folding and substrate binding, but fail to form a fluorescein binding pocket. But the fact that the fluorescein label is not far from the binding site, and that there is good agreement between steady-state binding parameters reported herein and those reported from catalytic activity studies, supports the notion that emission enhancement directly reflects substrate binding to a folded D1 molecule.

Chemical Modification Studies of Mg^{2+}-Dependent Folding. That substrate binding does not occur without Mg^{2+} is strongly supported by results from chemical modification footprinting followed by reverse transcription. Dimethyl sulfate (DMS) modifies the N1 of A and N3 of C not involved in Watson−Crick interactions, and this results in a stop in reverse transcription (Inouye & Cech, 1985). DMS modifications indicate that the EBS2 site in D1 is protected only in presence of substrate and Mg^{2+} (Figure 5a, lane 4), indicating that the EBS2·IBS2 helix forms only in the presence of Mg^{2+} and not K^+. The same modification patterns were observed in the EBS1 region (Figure 5b, lane 4). Chemical modification provides a direct structural demonstration that substrate binding is dependent on Mg^{2+} rather than K^+, and this type of analysis confirms results obtained by fluorescence studies. Furthermore, chemical modification experiments also showed a salt dependence for modification of tertiary structural elements within D1 (Figures 5 and 6), which further supports the idea that D1 exists in different conformations in K^+ vs Mg^{2+}. For example, positions 259C and 255C in the loop region of D2a, which are part of the so-called $\beta-\beta'$ paired element (Figure 6) (Michel & Ferat, 1995), are significantly more protected in Mg^{2+} (Figure 5a). For the first time, the data also show that some form of pairing actually extends on either side of the known $\beta-\beta'$ covariation. These results indicate that the formation of the long range $\beta-\beta'$ interaction requires Mg^{2+}, which further suggests that Mg^{2+} is required in the tertiary fold of D1. Also, in the loop region between D‴ and D″, several residues (Figure 6, positions 226−229) were more protected in Mg^{2+} (Figure 5a), suggesting that they are involved in an unidentified pairing or that they are sterically occluded in the tertiary structure. The highly conserved (Jacquier & Michel, 1987) and catalytically essential (Harris-Kerr et al., 1993) $\alpha-\alpha'$ interaction failed to form properly in the absence of Mg^{2+} (Figures 5b and 6). This is one of the main tertiary structural contacts required for assembly of the substrate binding site (P.Z.Q. and A.M.P., unpublished results). An effect that was apparent in all of these experiments was that residues flanking important tertiary structures, such as nucleotides at the edges of the $\beta-\beta'$ and EBS1/IBS1, became more susceptible to attack in the presence of Mg^{2+} (Figure 5). This suggests that these nucleotides have become more strained and exposed once the intron core had folded. It should be interesting to see how this structural transition is related to functions of D1.

Quantifying the Role of Magnesium in Folding and Substrate Binding of D1. Once it was established that Mg^{2+} is required for the folding of ribozyme, it was useful to study the effect of varying Mg^{2+} concentrations. Fixed concentrations of FAM-S (10 nM) and D1 (50 nM) were incubated separately under different Mg^{2+} concentrations, and then binding of substrate to ribozyme was initiated in the stopped-flow mixing chamber. Values for k_{obs} were extracted from the time traces and plotted against Mg^{2+} concentration (Figure 7). When [Mg^{2+}] was above 25 mM, k_{obs} was the same with or without K^+. However, at [Mg^{2+}] lower than 25 mM, high concentrations of K^+ quenched the fluorescent enhancement signals, presumably due to competition between K^+ and Mg^{2+}. In order to exclude this K^+ interference, subsequent experiments were done without K^+. Values of k_{obs} increased as [Mg^{2+}] increased (Figure 7a) and the percentage emission enhancement also increased as a function of [Mg^{2+}] (data not shown), indicating that more E·S complex forms as [Mg^{2+}] is raised.

From eq 2, the dependence of k_{obs} on [Mg^{2+}] can be separated into two parts: [E_{fold}] and the association/dissociation rate constants (k_{on} and k_{off}). Since only properly folded D1 is capable of binding substrate and enhancing fluorescence emission, k_{obs} depends on the folded D1 concentration, [E_{fold}], rather than just the total D1 concentration, [E]. The [E_{fold}] increases as [Mg^{2+}] increases, which results in the formation of more E·S complex and apparently tighter binding. The other components in k_{obs} are k_{off} and k_{on}. The Mg^{2+} dependence of k_{off} was measured by pulse−chase experiments at different [Mg^{2+}]: at 300 mM Mg^{2+}, the value of k_{off} was 0.43 ± 0.01 min^{-1}, while at 30 mM Mg^{2+}, the

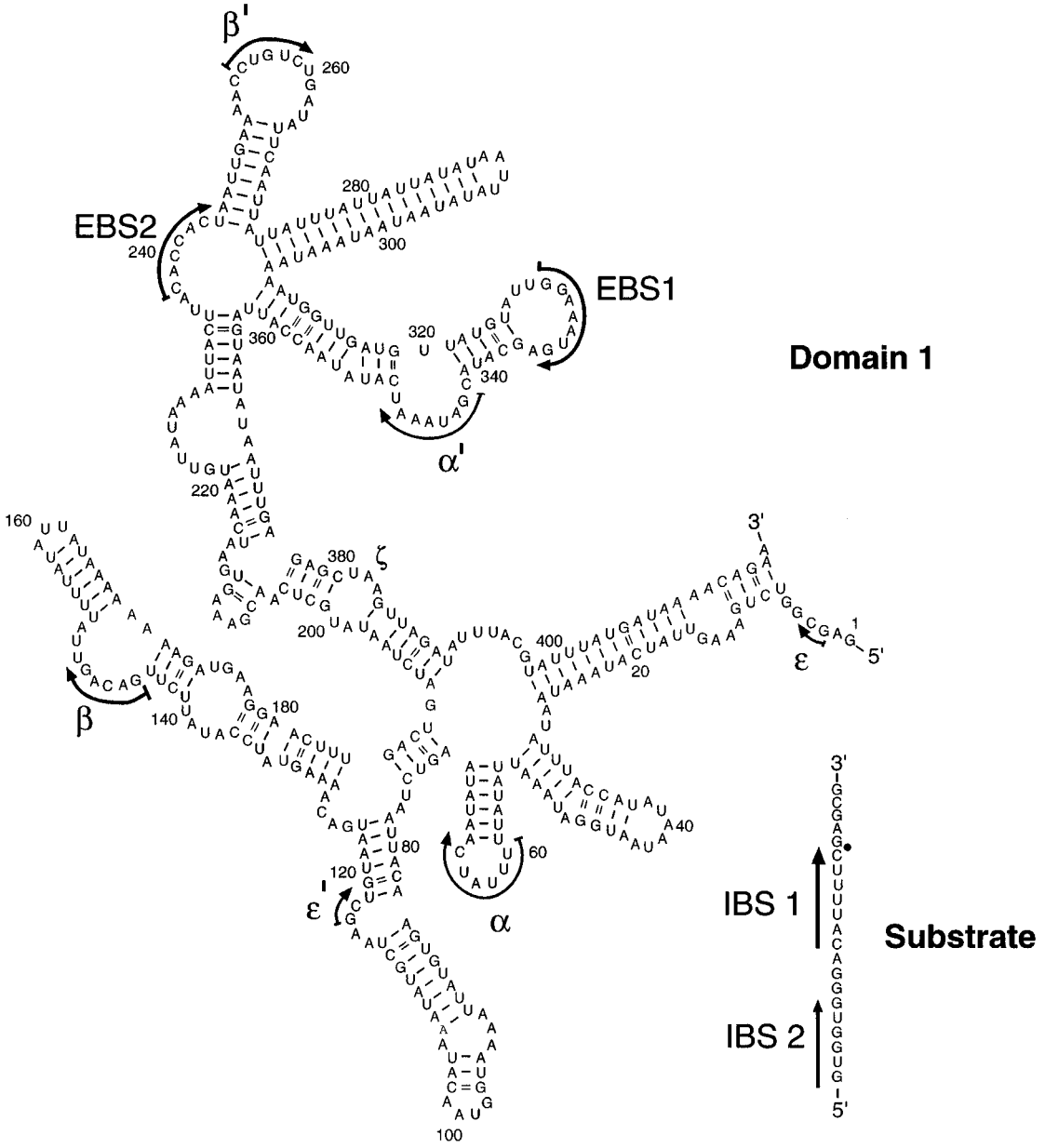

FIGURE 6: Secondary structure of domain 1. The secondary structure of D1 is shown (Jacquier & Michel, 1987), together with the known long-range tertiary interactions (Michel & Ferat, 1995). The IBS−EBS, α−α′, *β*−*β*′, and *ϵ*−*ϵ*′ interactions are highlighted, with arrows to indicate their polarity. The position of the *ζ*−D5 tertiary interaction is also indicated. Substrate is shown as a second molecule, with a dot indicating the site of cleavage. An *ϵ*−*ϵ*′ interaction does not form between S and D1, but the *ϵ*−*ϵ*′ interaction must be present within D1 in-cis, as shown here, or catalytic activity is severely disrupted (W. J. Michels, 1997). The D1 construct used in these studies extends to nucleotide 425 of the intron, although these are not required for activity.

value of k_{off} was 0.42 ± 0.02 min^{-1} (data not shown). This agreement in k_{off} over a 10-fold range in Mg^{2+} concentration strongly suggests that k_{off} is independent of [Mg^{2+}]. To a certain degree, it is difficult to distinguish the Mg^{2+} dependence of k_{on} from that of [E_{fold}] because increases in either [E_{fold}] or k_{on} will lead to apparent decreases in K_d. In addition, k_{on} could be coupled to E_{fold}, since a conformational change in E might affect the rate of substrate association. This type of effect might be expected in a system like the *Tetrahymena* ribozyme, where the overall rate of substrate binding reflects a combination of terms for duplex formation and subsequent docking (Bevilacqua et al., 1992). Nonetheless, modification interference data (Figure 5) show clearly that the folding of the ribozyme (and thus the [E_{fold}] term) is dependent on Mg^{2+}, while k_{on} is unlikely to be dependent on [Mg^{2+}] because it is at the known limit in rate for duplex formation. This limit (10^7−10^8 M^{-1} min^{-1}) varies little, despite the fact that it has been measured independently by different laboratories under many different salt conditions. Therefore, the evidence presented herein is consistent with a model in which [E_{fold}] is the Mg^{2+}-dependent term in the expression describing k_{obs} (eq 3). As such, the Mg^{2+} ions detected through fluorescence measurements of real-time substrate association are actually "folding" ions, which play major roles in the ribozyme tertiary structure, rather than just the association/dissociation rate constants.

On the basis of these arguments, a model was built to quantitatively analyze the [Mg^{2+}] dependence of k_{obs}. To this end, eq 2 was modified as shown below:

$$k_{obs} = k_{on}[E_{fold}] + k_{off} \quad (3)$$

In this expression, only [E_{fold}] is assumed to vary with

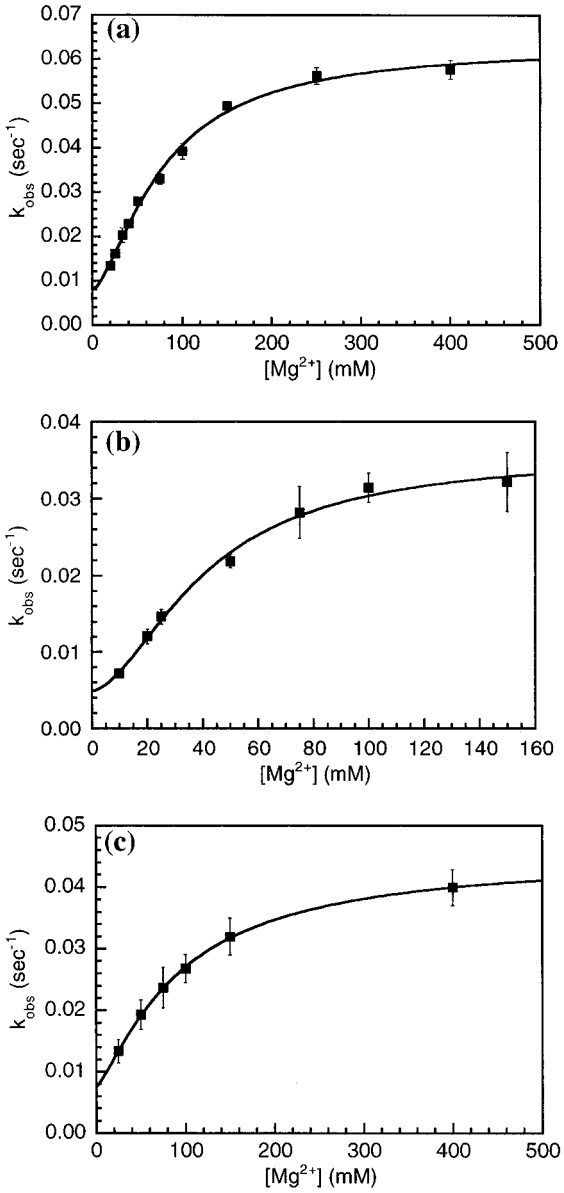

FIGURE 7: Dependence on Mg^{2+} of ribozyme folding and substrate binding. (a) Association rates between 10 nM FAM-S and 50 nM D1 were measured under various Mg^{2+} concentrations as described. Data were fit to eq 5, which gave $K_{Mg} = 78 \pm 7.3$ mM and $n = 1.5 \pm 0.3$. In fitting eq 5, k_{on} and k_{off} were included as Mg^{2+}-independent, floating variables. (b) Association rates between 10 nM FAM-S and 50 nM D13 were plotted against Mg^{2+} concentrations, and data were fit to eq 5. The value for $K_{Mg} = 41 \pm 5.3$ mM, with $n = 1.7 \pm 0.4$. (c) Association rates between 10 nM FAM-S and 50 nM D135 were plotted against Mg^{2+} concentrations, and data were fit to eq 5. The value for $K_{Mg} = 94 \pm 4.1$ mM, with $n = 1.3 \pm 0.2$.

$[Mg^{2+}]$, while k_{off} and k_{on} are treated as Mg^{2+}-independent variables.

Furthermore, interactions between D1 and magnesium can be described in Scheme 3,

Scheme 3

$$E + nMg^{2+} \rightleftharpoons E{\cdot}nMg^{2+}$$

where n represents the number of different magnesium ions involved in this process. This results in the following expression:

$$[E_{fold}] = [E] \frac{[Mg^{2+}]^n}{[Mg^{2+}]^n + K_{Mg}^{\,n}} \quad (4)$$

where K_{Mg} represents the apparent affinity for Mg^{2+} ions involved and n represents a lower limit for the number of ions involved and provides an index of cooperativity between Mg^{2+} binding sites (a Hill coefficient). Substituting eq 4 into eq 3, one obtains the $[Mg^{2+}]$ dependence of k_{obs}:

$$k_{obs} = k_{on}[E] \frac{[Mg^{2+}]^n}{[Mg^{2+}]^n + K_{Mg}^{\,n}} + k_{off} \quad (5)$$

Fitting the data to eq 5 (Figure 7a), the estimated values for D1 are $K_{Mg} = 78 \pm 7.3$ mM and $n = 1.5 \pm 0.3$. As n is a lower limit for the total number of bound Mg^{2+} ions, the data suggest that the folding process reflected in substrate binding involves at least two Mg^{2+} ions. The fact that $n > 1$ indicates that the ions bind cooperatively and the deviation of n from an integer value (1 or 2) may suggest that the Mg^{2+} ions involved do not bind with complete cooperativity. Because the k_{obs} measured in this case is dominated by terms that reflect the Mg^{2+}-dependent fraction of folded molecules, experimental measurements of k_{obs} provide information on the properties of specific associated metal ions.

Effect of Magnesium in Folding and Substrate Binding of D13 and D135. The data up to this point indicate that D1 functions as an independent folding unit with respect to substrate recognition. Other catalytically essential domains, such as D3 and D5, were observed to have little role in D1 folding or substrate binding. However, comparative K_d values were obtained under high salt conditions (1 M KCl, 0.1 M $MgCl_2$), and one might therefore argue that contributions from elements outside D1 are masked under this condition, since high ionic strength can compensate for loss of RNA structures. A better comparison might be made in the absence of KCl, using a range of Mg^{2+} concentrations, where differences in the folding of ribozyme derivatives could become apparent. Because it has been established that the Mg^{2+} dependence of k_{obs} reflects the Mg^{2+} dependence of ribozyme folding, one could monitor the Mg^{2+} dependence of substrate association with D13 and D135 in order to obtain further information on the role of catalytically essential domains in ground state folding.

To this end, the dependence of k_{obs} on $[Mg^{2+}]$ for D13 and D135 was measured in the absence of K^+, following the same experimental procedures as those used with D1. Similar to the D1 case, k_{obs} for both D13 and D135 increased as $[Mg^{2+}]$ increased. The values of k_{obs} are similar for all three ribozymes under the same Mg^{2+} concentrations (Figure 7b,c). When the data were fitted to eq 5, K_{Mg} was estimated to be 41 ± 5.3 mM for D13 and 94 ± 4.1 mM for D135, respectively. These values are similar to that of D1, indicating folding and substrate binding in all three ribozymes involve a process with similar Mg^{2+} requirements. Furthermore, n was estimated to be 1.7 ± 0.4 for D13, and 1.3 ± 0.2 for D135. Again, n values for all three ribozymes are very similar to each other, suggesting that all three ribozymes have the same number of magnesium ions involved in the folding process and the same degree of cooperativity among them.

Similarities in k_{obs}, K_{Mg}, and n for D1, D13, and D135 imply that these ribozymes use Mg^{2+} in analogous ways for

promoting folding and substrate binding. The apparent affinity for the Mg^{2+} sites, as well as the number of cooperative Mg^{2+} sites are very similar for all three ribozyme variants. Addition of catalytically essential domains does not relax the degree of magnesium dependence for D1 folding and substrate binding. This provides another piece of evidence that catalytically essential domains outside D1 have little influence on its folding. D1 itself is capable of folding into the correct tertiary structure to bind substrate.

DISCUSSION

Value of FAM-S as a Probe of Group II Intron Ribozyme Folding. It is always informative to monitor substrate binding independent of enzyme catalytic activity, but monitoring binding directly and in real time has particular advantages over equilibrium binding assays that depend on conventional separation techniques, many of which can affect the apparent off-rate of bound species, and have very limited windows of detection. Furthermore, if binding can be monitored in such a way that it directly reflects the folded state of the enzyme, varying reaction conditions can provide an abundance of additional information on conformational properties of the enzyme. The FAM-S probe provides a direct means for monitoring association and dissociation rate constants that has all of the advantages enumerated above.

When the binding of FAM-S is monitored, rather than the binding of unlabeled substrate, the emission signal reflects a change in the local environment around the fluorescein label, which correlates directly with the tertiary folding of D1. FAM-S therefore provides direct evidence that folding and substrate binding are strongly connected. Fluorescein tags on nucleic acids and other biomolecules have previously been reported to undergo environment-dependent changes in their luminescence intensity (Cooper & Hagerman, 1990; Lee et al., 1994; Livak et al., 1995). In the present case, time-dependent changes in fluorescence emission enhancement reflect the magnitude of substrate dissociation/association rate constants and the folded state of the ribozyme. By using FAM-S in conjunction with stopped-flow techniques, association and dissociation kinetics have been monitored in real time. From the apparent association rates (k_{obs}), one obtains not only K_d but also the individual rate constants k_{on} and k_{off}. Furthermore, since k_{obs} reflects the quantity of folded RNA molecules, it provides a way to determine the dependence of RNA folding on external factors, such as the concentration of added metal ions. Therefore, quantitative analysis of k_{obs} allows one to define the contributions of different factors in ribozyme folding.

In the present work, fluorescence studies of D1 folding were complemented by chemical modification studies in which the structure of D1 was examined directly. Chemical modification footprinting/reverse transcription revealed that there are different steady-state conformations of D1, depending on the presence of particular metal ions and on the addition of substrate (Figure 5). In all cases, the information from chemical modification footprinting was consistent with conclusions drawn from fluorescence studies using FAM-S. Time-dependent chemical modification studies would be particularly helpful in the future for revealing not only the different conformations of the ribozyme but also the transitions between conformations.

D1 Behaves as an Independent Folding Unit. The fact that D1 readily binds substrate in the absence of other domains suggests that D1 provides all of the contacts necessary for maintaining the normal amount of substrate binding energy. Furthermore, this result indicates that domains 3 and 5, despite their role in enhancing the chemical rate of catalysis, do not form ground-state contacts to the substrate and they do not aid in formation of the substrate (or exon) binding site within D1. With respect to those elements important for substrate recognition, the D1 molecule constitutes an independent folding unit. All of the elements that are essential for correctly configuring the substrate binding site are included within the D1 sequence.

That D1 is an independent folding unit with respect to substrate binding is supported by the Mg^{2+} dependence of D1 folding, which is the same as that of D13 and D135. Domains 3 and 5 play their most important roles in the transition state for chemical catalysis (Michels et al., 1997), and there is little evidence for their role in stabilizing the folds of intronic superstructure. This is consistent with the observation that in oligonucleotide cleavage assays, attachment of D3 in-cis affects the k_{chem}, but not K_d, of D5 or D1 (Michels & Pyle, 1995; Michels et al., 1997). In addition, a recent cross-linking study showed that D3 cross-linked within itself but not with D1 (Podar et al., 1995).

D1 as a Scaffold for Group II Intron Assembly. Group II introns differ from group I introns in that no catalytic core of nucleotides is evident from the location of phylogenetically conserved residues in the secondary structure (Michel et al., 1989). There are few conserved nucleotides in group II introns and no phylogenetic covariations in base pairing between any of the six group II intron domains (Michel et al., 1989). The few Watson−Crick covariations that exist occur across the secondary structure of D1 (Figure 6). The overall form of the secondary structure in group II introns is relatively conserved, however, suggesting that the architecture and placement in space of the covarying base pairs are critical for the folded structure.

D1 is the largest intronic domain, it recognizes the 5′-exon (or oligonucleotide substrates when presented in-trans) and contains the covarying α−α′, β−β′, and ϵ−ϵ′ elements within it (Michel et al., 1989). Therefore, D1 is the best candidate to serve as a type of core for intron folding. However, the sense in which it serves as a core is different from the tightly packed nucleation centers revealed in studies of other ribozymes. Rather than a core, D1 is more likely to provide a scaffold on which the other domains are hung. Within D1, the covarying elements that pair with each other (notably α−α′ and β−β′) are located quite far apart from each other in the span of secondary structure. With the addition of Mg^{2+}, these distal contacts are made and provide apparent anchor points for the overall architecture of D1. Once tertiary interactions form within D1, one can envision that the final folded structure of D1 looks like an open lattice that contains large holes or pockets for the association of other domains. The other domains probably do not alter the overall folding of D1, although each local pocket of D1 might adapt through induced fit. With all domains placed in the correct positions, interdomain contacts could form rapidly, locking the intron into a folded structure.

One might ask whether all of the group II intron domains, as defined by phylogenetic analysis and apparent secondary structure, are actually independent folding units or if their folding processes are inter-related? Of the six domains, domain 2 (D2) and domain 4 (D4) have little conservation

throughout the group II intron family. Although there is evidence for a poorly-conserved interaction between D2 and D6, many studies have shown that self-splicing introns retain most of their activity when D2 and D4 are deleted (V. T. Chu, Q. Liu, A. M. Pyle, manuscript in preparation; Kwakman et al., 1989; Koch et al., 1992). Because only D1, D3, D5, and D6 are strictly required for the functions of the intron, only they will be taken into account when considering the architecture of the group II intron catalytic core. Since D3, D5, and D6 are relatively small, the local folding of each may represent simple processes that occur rapidly and independently of one another. Data presented here suggest that the ground-state folding of D1 is also independent of other domains. Thus, it is likely that the first step of the group II intron folding is the local folding of the individual domains, which then coalesce upon the D1 lattice to form the catalytic core of the intron.

This folding framework immediately leads to two important questions. First, what are the internal elements that control D1 folding and what are their individual roles in defining the D1 folding pathway? Data presented here indicate that folding of D1 is controlled by several internal elements (the EBS/IBS interactions, α−α′ and *β*−*β*′) and that these elements require Mg^{2+} for tertiary contact formation. Additional points of contact must exist within D1, and it will be especially important to identify these through additional experiments. The second question is, how do other domains interact with D1? There is evidence that the GAAA tetraloop in D5 docks into a conserved stem−loop structure in D1 (Costa & Michel, 1995). But this constitutes only one of several anchor points that are required between these two domains, since D5 contains many atoms that form tertiary contacts and most of these do not involve the tetraloop (Abramovitz et al., 1996; B. B. Konforti, D. L. Abramovitz, L. Beigelman, and A. M. Pyle, manuscript in preparation). Finally, it is important to determine if docking of other domains induces changes in the tertiary folding of D1. Chemical modification and fluorescence resonance energy transfer (FRET) experiments are promising approaches for resolving these issues.

Role of Mg^{2+} in the Folding of D1. In the process of RNA folding, metal ions, and Mg^{2+} in particular, often play a critical role (Pan et al., 1993; Pyle, 1993, 1995). Besides screening the negative charges of the nucleic acid backbone, metal ions also mediate the structural organization of many RNA molecules (Saenger, 1984). Mg^{2+} is now known to be important for the tertiary folding of all large ribozymes. It has been shown that RNA folding can be manipulated by controlling magnesium concentrations, and various degrees of Mg^{2+} dependence have been used to dissect certain RNA folding pathways (Celander & Cech, 1991; Laggerbauer et al., 1994; Zarrinkar & Williamson, 1994; Beebe et al., 1996). Furthermore, metal ion dependence has been used as an important measure of the structural integrity of RNA domains. However, since Mg^{2+} functions in both folding and catalysis, it has not been possible to distinguish these two roles through experiments that only measure catalytic activity. Until now, independent evidence for a Mg^{2+} role in folding of group II intron ribozymes was unavailable. By taking advantage of the fact that folding of D1 can be monitored in the absence of other catalytic essential components, the present study has provided evidence that specific metal ions are required in the formation of ground-state ribozyme structure.

Data from fluorescence investigations and chemical modification indicate that D1 exists in different conformations under different ionic conditions. Mg^{2+} is required and sufficient for the tertiary structure formation, in which long-range interactions are formed. It is also required for the formation of local structure that results in emission enhancement by the fluorescein attached to substrate. Despite its large effect on the rate of catalysis, K^+ seems to be dispensable for tertiary structure formation. It is highly significant that elements of D1 tertiary structure cannot form and that substrate cannot bind in the presence of K^+. The result is surprising because the concentrations of KCl used in these experiments are high enough to promote simple duplex formation (Schildkraut & Lifson, 1968; Williams et al., 1989) and the substrate−D1 interaction, the α−α′ interaction, and the *β*−*β*′ interaction are each composed of duplexes. If substrate binding consisted only of the formation of simple duplexes between the IBS regions of substrate and flexibly connected EBS regions on the intron, then K^+ would be sufficient for promoting substrate association. The fact that it is not sufficient supports an underlying hypothesis that D1 folding into a discrete tertiary architecture is required for base pairs to form between substrate and D1, and between the *β*−*β*′ and α−α′ elements. This tertiary structure depends on association of specific Mg^{2+} ion(s).

Folding and Substrate Binding Require Specific Mg^{2+} Ions. Using stopped-flow fluorescence techniques, we have shown that the Mg^{2+} dependence of ribozyme folding can be revealed through analysis of Mg^{2+}-dependent substrate association rates (k_{obs} values). The Mg^{2+} ions detected in this analysis are actually "folding" ions rather than ions that contribute directly to the k_{on} or k_{off} terms describing substrate interaction with the ribozyme. This finding is consistent with the idea that substrate binding is not simply the result of simple duplex formation, but depends on a particular, Mg^{2+}-dependent ribozyme fold. The sheer magnitude of the apparent Mg^{2+} binding affinities (41−94 mM) supports this notion, since the Mg^{2+} concentrations required for simple charge screening in duplexes (Williams et al., 1989), and even in large ribozymes (Celander & Cech, 1991; Beebe et al., 1996), is relatively low (1−10 mM). However, charge screening effects would not be expected to enter into this analysis because substrate and ribozyme had each been incubated with Mg^{2+} prior to stopped-flow measurements of their association.

The number of specific Mg^{2+} ions (n), or classes of ions, involved in the folding and substrate binding was estimated to be at least two. There are probably other Mg^{2+} ions that are not reflected through the substrate binding process, especially those involved in interactions between D1 and other domains. The specific Mg^{2+} ions detected in this study have rather weak apparent binding affinities, with apparent K_{Mg} values ranging between 41 and 94 mM for D1, D13, and D135. While this may represent truly weak Mg^{2+} association, the large apparent K_{Mg} values may instead indicate that Mg^{2+} binding to specific sites is coupled to other processes, such as ribozyme folding. This would be consistent with similar effects observed in studies of other ribozymes (Zarrinkar & Williamson, 1994; Beebe et al., 1996). Under such circumstances, Scheme 3 would be expanded as shown in Scheme 4, where n represents

Scheme 4

$$\begin{array}{ccc} nMg^{2+} + E_{unfold} & \overset{K'_{fold}}{\rightleftharpoons} & nMg^{2+} + E_{fold} \\ \Downarrow & & \Uparrow \; K'^{n}_{Mg} \\ E_{unfold} \bullet nMg^{2+} & \rightleftharpoons & E_{fold} \bullet nMg^{2+} \end{array}$$

specifically-bound Mg^{2+} (rather than those involved in charge-screening), and the apparent Mg^{2+} affinity is composed of two terms:

$$K^{n}_{Mg} = K'^{n}_{Mg}(1 + K'_{fold}) \quad (6)$$

Given this relationship, a large unfavorable K'_{fold} term would lead to a weak apparent K_{Mg}. Using the methodology described in this manuscript, one cannot experimentally distinguish this more complex model from the simple one described earlier in Scheme 3. However, the detailed picture of ribozyme folding and its relationship to specific Mg^{2+} sites is an interesting subject for further study. It may be significant that the Mg^{2+} sites discovered here are similar in apparent affinity to the weak Mg^{2+} involved in the binding of RNase P and tRNA (Beebe et al., 1996). However, the weak ions studied in the case of RNase P were specifically involved in effects on k_{off} for the RNaseP−tRNA complex rather than the fraction of folded ribozyme as in the work presented here.

The apparent weakness of the Mg^{2+} binding observed here might seem contradict the fact that certain group II ribozymes can function at low magnesium concentrations (Michels, 1997). However, those particular ribozyme variants are highly efficient, with chemical steps that are no longer rate-limiting for the overall reaction. Their apparent activity at low Mg^{2+} is unlikely to represent optimal activity. In these cases, chemical catalysis is already so fast that any diminution in rate is obscured by other rate-limiting processes such as duplex formation and conformational changes that can still occur at lower Mg^{2+}. It is likely that group II introns function with the aid of associated proteins in-vivo (Lambowitz & Perlman, 1990). This is known to be the case for group II introns that associate with their own encoded proteins (D4 often contains an open reading frame) (Perlman & Butow, 1989; Zimmerly et al., 1995; Yang et al., 1996). As in the case of C5 protein and RNase P (Reich et al., 1988), group II intron-associated proteins may lower metal ion requirements for conformational change and folding.

SUMMARY AND OUTLOOK

D1 is among the most complex components of any catalytic RNA known, and its mode of folding is difficult to understand and to study. Fluorescence techniques provide a means for monitoring the spatial and temporal behavior of this large RNA, and the studies presented herein represent the first example of this analysis on group II introns. They show that D1 folds independently of other intronic domains, thus simplifying the larger problem of group II intron folding and providing a working model for the group II intron folding pathway. They also demonstrate that specific Mg^{2+} ions are intimately involved in the tertiary structure formation of D1.

Although certain aspects of D1 folding are elucidated by the work presented herein, the problem of D1 folding is substantially more complex than anything that can be revealed using FAM-S alone. A single fluorophore placed on the substrate will report on the local environment around the substrate binding site. But since D1 itself does not have catalytic capability (in the absence of D5), it is unlikely that information gained from a substrate label will represent all of the folding events important for assembly of the active site. Catalytic function of group II introns requires that D1 also interact with other domains, such as D3 and D5 (Koch et al., 1992; Pyle & Green, 1994; Michels & Pyle, 1995; Podar et al., 1995). In addition, the slow on-rate for substrate binding is likely to mask other processes, such as conformational change in D1. To monitor these events, further studies will require that fluorescent tags be placed within D1 and on other domains. Double labeling D1 with two fluorophores and following their interactions by fluorescent resonance energy transfer (FRET) will be particularly useful for tracking conformational change and elucidating the folding pathway. Accompanied by chemical modification studies, real-time spectroscopic studies of group II intron folding represent a particularly promising approach for monitoring the dynamic behavior of this uniquely complex ribozyme.

ACKNOWLEDGMENT

We thank Justin B. Green, Dana L. Abramovitz, Boyana B. Konforti, and Eckhard Jankowsky for helpful comments on the manuscript. In addition, we are grateful to a reviewer for bringing the coupled equilibria presented in Scheme 4 to our attention. We thank Qiaolian Liu for constructing the plasmid pT7D135 and William J. Michels for constructing plasmid pT7D13.

REFERENCES

Abramovitz, D. L., Friedman, R. A., & Pyle, A. M. (1996) *Science 271*, 1410−1413.
Beebe, J. A., Kurz, J. C., & Fierke, C. A. (1996) *Biochemistry 35*, 10493−10505.
Bevilacqua, P. C., Kierzek, R., Johnson, K. A., & Turner, D. H. (1992) *Science 258*, 1355−1358.
Cate, J. H., Gooding, A. R., Podell, E., Zhou, K., Golden, B. L., Kundrot, C. E., Cech, T. R., & Doudna, J. A. (1996) *Science 273*, 1678−1685.
Celander, D. W., & Cech, T. R. (1991) *Science 251*, 401−407.
Chanfreau, G., & Jacquier, A. (1994) *Science 266*, 1383−1387.
Cooper, J. P., & Hagerman, P. J. (1990) *Biochemistry 29*, 9261−9268.
Costa, M., & Michel, F. (1995) *EMBO J. 14*, 1276−1285.
Doudna, J. A., & Cech, T. R. (1995) *RNA 1*, 36−45.
Doudna, J. A., Couture, S., & Szostak, J. W. (1991) *Science 251*, 1605−1608.
Draper, D. E. (1996) *Nat. Struct. Biol. 3*, 397−400.
Eigen, M., & Hammes, G. G. (1963) *Adv. Enzymol. 25*, 1−38.
Fersht, A. (1985) *Enzyme Structure and Mechanism*, pp 128−132, W. H. Freeman, New York.
Griffin, E. A., Qin, Z.-F., Michels, W. A., & Pyle, A. M. (1995) *Chem. Biol. 2*, 761−770.
Harris-Kerr, C. L., Zhang, M., & Peebles, C. L. (1993) *Proc. Natl. Acad. Sci. U.S.A. 90*, 10658−10662.
Herschlag, D., & Cech, T. R. (1990) *Biochemistry 29*, 10159−10171.
Heus, H. A., & Pardi, A. (1991) *J. Mol. Biol. 217*, 113−124.
Inouye, T., & Cech, T. R. (1985) *Proc. Natl. Acad. Sci. U.S.A. 82*, 648−652.
Jacquier, A., & Michel, F. (1987) *Cell 50*, 17−29.

Johnson, K. A. (1992) Transient-state kinetic analysis of enzyme reaction pathways, in *The Enzymes*, 3rd ed., pp 1−61, Academic Press, Inc., San Diego, CA.
Kayne, M. S., & Cohn, M. (1974) *Biochemistry 13*, 4159−4165.
Kierzek, R., Turner, D. H., & Bevilacqua, P. C. (1993) *J. Am. Chem. Soc. 115*, 4985−4992.
Koch, J. L., Boulanger, S. C., Dib-Hajj, S. D., Hebbar, S. K., & Perlman, P. S. (1992) *Mol. Cell. Biol. 12*, 1950−1958.
Kunkel, T. A., Bebenek, K., & McClary, J. (1991) *Methods Enzymol. 204*, 125−139.
Kwakman, J. H. J. M., Konings, D., Pel, H. J., & Grivell, L. A. (1989) *Nucleic Acids Res. 17*, 4205−4216.
Laggerbauer, B., Murphy, F. L., & Cech, T. R. (1994) *EMBO J. 13*, 2669−2676.
Lakowicz, J. R. (1983) *Principles of Fluorescence Spectroscopy*, Plenum Press, New York.
Lambowitz, A. M., & Perlman, P. S. (1990) *Trends Biochem. Sci. 15*, 440−444.
Lee, S. P., Porter, D., Chirikjian, J. G., Knutson, J. R., & Han, M. K. (1994) *Anal. Biochem. 220*, 377−383.
Leonard, N. J., & Tolman, G. L. (1975) *Ann. N.Y. Acad. Sci. 255*, 43−58.
Livak, K. J., Flood, S. J. A., Marmoro, J., Giusti, W., & Deetz, K. (1995) *PCR Methods Appl. 4*, 357−362.
Michel, F., & Westhof, E. (1990) *J. Mol. Biol. 216*, 585−610.
Michel, F., & Ferat, J.-L. (1995) *Annu. Rev. Biochem. 64*, 435−461.
Michel, F., Umesono, K., & Ozeki, H. (1989) *Gene 82*, 5−30.
Michels, W. J. (1997) Ph.D. Thesis, Columbia University, New York.
Michels, W. J., & Pyle, A. M. (1995) *Biochemistry 34*, 2965−2977.
Milder, S. J., Weiss, P. S., & Kliger, D. S. (1989) *Biochemistry 28*, 2258−2264.
Murphy, F. L., & Cech, T. R. (1993) *Biochemistry 32*, 5291−5300.
Nelson, J. W., & Tinoco, I. J. (1981) *Biochemistry 21*, 5289−5295.
Pan, T. (1995) *Biochemistry 34*, 902−909.
Pan, T., Long, D. M., & Uhlenbeck, O. C. (1993) Divalent metal ions in RNA folding and catalysis, in *The RNA World*, pp 271−302, Cold Spring Harbor Laboratory Press, Plainview, NY.
Perlman, P. S., & Butow, R. A. (1989) *Science 246*, 1106−1109.
Pley, H. W., Flaherty, K. M., & McKay, D. B. (1994) *Nature 372*, 68−74.
Podar, M., Dib-Hajj, S., & Perlman, P. S. (1995) *RNA 1*, 828−840.
Porschke, D., & Eigen, M. (1971) *J. Mol. Biol. 62*, 361−381.
Pyle, A. M. (1993) *Science 261*, 709−714.
Pyle, A. M. (1995) The role of metal ions in ribozymes, in *Metal Ions in Biological Systems*, Marcel Dekker, Inc., New York (in press).
Pyle, A. M. (1996) Catalytic reaction mechanisms and structural features of group II intron ribozymes, in *Nucleic Acids and Molecular Biology*, pp 75−107, Springer-Verlag, New York.
Pyle, A. M., & Green, J. B. (1994) *Biochemistry 33*, 2716−2725.
Pyle, A. M., & Green, J. B. (1995) *Curr. Opin. Struct. Biol. 5*, 303−310.
Pyle, A. M., Murphy, F. L., & Cech, T. R. (1992) *Nature 358*, 123−128.
Reich, C., Olsen, G. J., Pace, B., & Pace, N. R. (1988) *Science 239*, 117−232.
Saenger, W. (1984) *Principles of Nucleic Acid Structure*, Springer-Verlag, New York.
Schildkraut, C., & Lifson, S. (1965) *Biopolymers 3*, 195−208.
Shalitin, N., & Feitelson, J. (1976) *Biochemistry 15*, 2092−2097.
Smith, D., Burgin, A. B., Haas, E. S., & Pace, N. R. (1992) *J. Biol. Chem. 267*, 2429−2436.
Tuschl, T., Gohlke, C., Jovin, T. M., Westhof, E., & Eckstein, F. (1994) *Science 266*, 785−789.
Uhlenbeck, O. C. (1995) *RNA 1*, 4−6.
van der Horst, G., Christian, A., & Inoue, T. (1991) *Proc. Natl. Acad. Sci. U.S.A. 88*, 184−188.
Varani, G., Aboul-ela, F., & Allain, F. H. T. (1996) *Prog. Nucl. Magn. Reson. Spectrosc. 29*, 51−127.
Williams, A. P., Longfellow, C. E., Freier, S. M., Kierzek, R., & Turner, D. H. (1989) *Biochemistry 28*, 4283−4291.
Wincott, F., DiRenzo, A., Shaffer, C., Grimm, S., Tracz, D., Workman, C., Sweedler, D., Gonzalez, C., Scaringe, S., & Usman, N. (1995) *Nucleic Acids Res. 23*, 2677−2684.
Wolfson, J. M., & Kearns, D. R. (1975) *Biochemistry 14*, 1436−1444.
Yang, J., Zimmerly, S., Perlman, P. S., & Lambowitz, A. M. (1996) *Nature 381*, 332−335.
Zarrinkar, P. P., & Williamson, J. R. (1994) *Science 265*, 918−924.
Zimmerly, S., Guo, H., Eskes, R., Yang, J., Perlman, P. S., & Lambowitz, A. M. (1995) *Cell 83*, 529−538.

BI962665C